The Analytical Force Prediction and Dynamic Response Analysis of the Bristol H25A Compressor

by

Zhijun Zheng

Thesis submitted to the Faculty of the
Virginia Polytechnic Institute and State University
in Partial Fulfillment of the Requirement for the Degree of

Master of Science
in
Mechanical Engineering

APPROVED:

Dr. Reginald G. Mitchiner, Chairman

Dr. Larry D. Mitchell

Dr. Charles E. Knight

December, 1995

Blacksburg, Virginia

The Analytical Force Prediction and Dynamic Response Analysis of the Bristol H25A Compressor

by

Zhijun Zheng

Dr. Reginald G. Mitchiner, Chairman

Mechanical Engineering

(ABSTRACT)

The objective of this research is to perform an in-depth study of the force components within the H25A compressor along with a computer simulation program and the dynamic response analysis of the compressor internals using the finite element method.

The model for force prediction was created based on the assumption that the frame of the shell structure is rigid and the subassemblies within the shell behave as one lumped mass. Springs are the connections between the shell and the subassemblies. Various parameters of the model were entered through the preprocessor of the simulation program which provides a series of data entry forms. The processor part of the program contains several modules for performing different tasks, such as the eigenanalysis, kinematic force computation, displacement/velocity/acceleration prediction, spring-end force calculation and variable-speed motor simulation. The simulation program also features post-processor functions in order to display the results of the analysis in plots, tables or with animation.

Further research was focused on the correlation of the predicted force and orbit with the observations. With a finite element model of the full compressor, the spring-end forces due to the excitation at mass center were obtained from the dynamic response analysis and compared to the force gauge measurements. The excitations included the enforced displacement at the mass center which was regenerated from the accelerometer measurements, and the superposition of the kinematic forces and equivalent valve impact forces at the mass center.

To Lisa

ACKNOWLEDGMENTS

I would like to thank my advisor Dr. R. G. Mitchiner, for the unmeasurable amount of support and guidance provided not only for this thesis, but through out my graduate study. I would also express my thanks to Dr. L. D. Mitchell and Dr. C. E. Knight for serving on my graduate committee, and for their suggestions on this research.

I also would like to thank Bristol Compressors, Inc. and the Virginia Center for Innovative Technology for there sponsorship of this project.

I would like to acknowledge other team members for their assistance on this project: Ramakant Arcot, Anand Ramani, Matthew Craun, Jay Rose, Hugo Camargo, Samir Singh, and Robert Estep.

Finally, I would like to thank my wife Lisa for her encouragement, support, and most of all, love.

Table of Contents

Table of Contents ..... **v**

List of Figures ..... **ix**

List of Tables ..... **xiii**

1. Introduction **1**

1.1 Project Overview 1

1.2 The Bristol H25A Compressor 3

1.3 Previous Analysis Results 3

2. Theoretical Model **8**

2.1 Establish the System Equations of Motion 8

2.2 Evaluation of the Parameters in the System Equations of Motion 9

2.2.1 System Mass and Inertia Matrix 9

2.2.2 System Gyroscopic Matrix 11

2.2.3 System Stiffness Matrix 12

2.2.4 Shaking Forces and Moments Vector 14

2.3 Solution of the System Equation of Motion 14

3. Processor **16**

3.1 Eigenvalue and Eigenvector Problems 16

3.1.1 Natural Frequencies and Normal Modes 16

3.1.2 Solving for Eigenvalue and Eigenvector Problems 17

3.2 Forward and Inverse Fourier Transforms 18

3.3 State Vector Method for Solving the System with Gyroscopic Matrix 19

3.3.1 Introduction of the State Vector Method 20

3.3.2 State Vector Solution for Gyroscopic System 20

3.3.2.1 State Vector 20

3.3.2.2	Free Vibration	21
3.3.2.3	Forced Vibration	23
3.3.2.4	Illustrative Example of the State Vector Solution	24
3.3.2.5	Applying the State Vector Method to the Compressor Model	26
3.4	Modal Matrix Method	40
3.4.1	Orthogonality of Eigenvectors	40
3.4.2	Modal Matrix	41
3.4.3	Decoupling Forced Vibration Equations	42
3.5	Displacement, Velocity and Acceleration Calculation	43
3.6	Spring-End Force/Moment Calculation	47
3.7	Variable Speed Motor Simulation	47
3.8	Effects of Valve Impact	48
3.8.1	Motion of the Discharge and Suction Valves During Operation	48
3.8.2	Derivation of the Impact Force for the Second Cylinder from the Single Cylinder Model	49
3.8.3	Equivalent Forces and Moments at the Mass Center	51
4.	**Preprocessor and Post Processor**	**53**
4.1	Introduction	53
4.2	Preprocessor	53
4.2.1	Menu Structures	53
4.2.2	Forms and Their Features	55
4.2.2.1	Compressor/Common Variables/Pressure Form	56
4.2.2.2	Compressor/Common Variables/Crank Form	57
4.2.2.3	Compressor/Common Variables/Connecting Rod Form	57
4.2.2.4	Compressor/Common Variables/Pistons & Cylinders Form	58
4.2.2.5	Compressor/Common Variables/Counter Weight Form	59
4.2.2.6	Compressor/Cylinder Variables Form	59
4.2.2.7	Mounts/Number of Mounts Form	60
4.2.2.8	Mounts/Locations Form	61

4.2.2.9 Mounts/Stiffnesses Form and Mount Dampers Form 61
4.2.2.10 Mass Properties Form 62
4.2.2.11 Motor Parameters Form 63
4.2.2.12 Motor Parameters/Tolerance for Steady State Form 63
4.3 Post Processor 64
4.3.1 Menu Structures 65
4.3.2 Forms and Their Features 65
4.3.2.1 Eigen Analysis Form 66
4.3.2.2 Normal Modes Animation Form 66
4.3.2.3 Force Analysis (Plotting) Form 67
4.3.2.4 Orbit Analysis (Plotting) Form 68
4.3.2.5 Orbit Analysis (Animation) Form 69
4.3.2.6 Displacement/Velocity/Acceleration Analysis (Plotting) Form 69
4.3.2.7 Spring-End Force Analysis (Plotting) Form 71
4.3.2.8 Variable Speed Motor Analysis (Plotting) Form 71
4.3.2.9 Numerical Data Display Forms 72
4.4 Additional Features 73
4.4.1 Tool Bar 73
4.4.2 Print and Print Preview Functions 73
4.4.3 On-Line Help System 76

5. Mass Center Dynamics 77
5.1 Measured Acceleration Data 78
5.2 Finding the Break Point of Two Periods of Data 81
5.3 Regeneration of the Acceleration at the Mass Center of Gravity 87

6. Finite Element Analysis 99
6.1 General Procedure for Obtaining the Force at the Spring-End 99
6.2 Spring-End Force and Moment Analysis by Mass Center Acceleration

Input Using the Original Finite Element Model 102
6.3 Spring-End Force and Moment Analysis by Mass Center Acceleration Input Using the Instrumented Finite Element Model 106
6.4 Investigation of Local Resonances 131
6.5 Spring-End Force and Moment Analysis by Mass Center Force Input Using the Instrumented Finite Element Model 137

7.0 Conclusions and Recommendations 142
7.1 Conclusions 142
7.2 Recommendations 144

References 146
Vita 148

List of Figures

Figure 1.1	The Bristol H25A Compressor	3
Figure 1.2	Internal Components of the Bristol H25A Compressor	4
Figure 1.3	The Bristol H25A Compressor Instrumentation	6
Figure 2.1	A Sketch of the Compressor Model	9
Figure 2.2	Origins of the Coordinate System Used by Arcot [3] and *COMP* ..	10
Figure 3.1a	Sine and Cosine Coefficient of the Force Vectors (Forces)	27
Figure 3.1b	Sine and Cosine Coefficient of the Force Vectors (Moments)	29
Figure 3.2a	Real Component of the Sine and Cosine Coefficient of the Displacements	35
Figure 3.2b	Real Component of the Sine and Cosine Coefficient of the Rotations	36
Figure 3.3	Response at the Mass Center in the Time Domain	39
Figure 3.4	The Difference in Rotation about the Rotor (Z) Axis Solved by Decoupling Method and State Vector Method (in percentage) vs. Crank Angle	39
Figure 3.5	Translational Displacement in the X Direction in the Frequency Domain, Sine, Cosine and Magnitude Plot	44
Figure 3.6	Translational Displacement in X Direction in the Time Domain, One Period	45
Figure 3.7	The xyz System and XYZ System	46
Figure 3.8	Piston and Valve Positions from Phase 1 to Phase 6	50
Figure 4.1	Pressure Input Form	57
Figure 4.2	Crank Input Form	57

Figure 4.3	Connecting Rod of Bristol H25A Compressor	58
Figure 4.4	Connecting Rod Input Form	58
Figure 4.5	Pistons & Cylinders Input Form	59
Figure 4.6	Counter Weight Input Form	60
Figure 4.7	Cylinder Variables Input Form	60
Figure 4.8	Number of Mounts Input Form	61
Figure 4.9	Locations Input Form	61
Figure 4.10	Mount Stiffnesses Input From	62
Figure 4.11	Mass Properties Input Form	63
Figure 4.12	Motor Parameters Input Form	64
Figure 4.13	Tolerance for Steady State Input Form	64
Figure 4.14	Eigenanalysis form	66
Figure 4.15	Normal Modes Animation Form	67
Figure 4.16	Force Analysis (Plotting) Form	68
Figure 4.17	Orbit Analysis (Plotting) Form	69
Figure 4.18	Orbit Analysis (Animation) Form	70
Figure 4.19	Displacement/Velocity/Acceleration Analysis (Plotting) Form	70
Figure 4.20	Spring End Force Analysis (Plotting) Form	71
Figure 4.21	Variable Speed Motor Analysis (Plotting) Form	72
Figure 4.22	Force Analysis (Data) Form	73
Figure 4.23	Standard Tool Bar in Main Form	74
Figure 4.24	Print Form	74
Figure 4.25	Print Preview Form	75
Figure 4.26	Help System Window	76
Figure 5.1	Measured Acceleration at Crank Case, Time Domain	79
Figure 5.2	Measured Acceleration at Motor-Cap, Time Domain	80
Figure 5.3	Break Point of Two Periods of Data	81
Figure 5.4	Measured Acceleration at Crank-Case, One Period	83

Figure 5.5	Measured Acceleration at Motor Cap, One Period	84
Figure 5.6	Measured Acceleration at Crank Case, Frequency Domain	85
Figure 5.7	Measured Acceleration at Motor Cap, Frequency Domain	86
Figure 5.8	Main Form of *OPTIMIZE*	92
Figure 5.9a	Regenerated Mass Center Acceleration in the Time Domain, Translational	95
Figure 5.9b	Regenerated Mass Center Acceleration in the Time Domain, Rotational	96
Figure 5.10a	Regenerated Mass Center Acceleration in the Frequency Domain, Translational	97
Figure 5.10b	Regenerated Mass Center Acceleration in the Frequency Domain, Rotational	98
Figure 6.1	Finite Element Model of the Full Compressor (Original)	100
Figure 6.2	Finite Element Model of the Subassemblies within the Compressor	101
Figure 6.3a	Regenerated Left Spring-End Force in the X Direction.....	107
Figure 6.3b	Regenerated Left Spring-End Force in the Y Direction.....	108
Figure 6.3c	Regenerated Left Spring-End Force in the Z Direction.....	100
Figure 6.3d	Regenerated Left Spring-End Moment about the X Direction.....	110
Figure 6.3e	Regenerated Left Spring-End Moment about the Y Direction.....	111
Figure 6.3f	Regenerated Left Spring-End Moment about the Z Direction.....	112
Figure 6.4a	Regenerated Right Spring-End Force in the X Direction.....	113
Figure 6.4b	Regenerated Right Spring-End Force in the Y Direction.....	114
Figure 6.4c	Regenerated Right Spring-End Force in the Z Direction.....	115
Figure 6.4d	Regenerated Right Spring-End Moment about the X Direction.....	116
Figure 6.4e	Regenerated Right Spring-End Moment about the Y Direction.....	117
Figure 6.4f	Regenerated Right Spring-End Moment about the Z Direction.....	118
Figure 6.5a	Regenerated Top Spring-End Force in the X Direction.....	119
Figure 6.5b	Regenerated Top Spring-End Force in the Y Direction.....	120

Figure 6.5c	Regenerated Top Spring-End Force in the Z Direction.....	121
Figure 6.5d	Regenerated Top Spring-End Moment about the X Direction.....	122
Figure 6.5e	Regenerated Top Spring-End Moment about the Y Direction.....	123
Figure 6.5f	Regenerated Top Spring-End Moment about the Z Direction.....	124
Figure 6.6a	Regenerated Shock-loop End Force in the X Direction.....	125
Figure 6.6b	Regenerated Shock-loop End Force in the Y Direction.....	126
Figure 6.6c	Regenerated Shock-loop End Force in the Z Direction.....	127
Figure 6.6d	Regenerated Shock-loop End Moment about the X Direction.....	128
Figure 6.6e	Regenerated Shock-loop End Moment about the Y Direction.....	129
Figure 6.6f	Regenerated Shock-loop End Moment about the Z Direction.....	130
Figure 6.7	Modeling the Force Gauge at the Top Spring	131
Figure 6.8	Top View of the General Electric Stator	133
Figure 6.9	Muffler Assembly	134
Figure 6.10	Shock-Loop	135
Figure 6.11	Finite Element Model of the Muffler/Shock-Loop Assembly	136
Figure 6.12	Vertical Vibration of the Muffler/Shock-loop Assembly	138
Figure 6.13	Twisting Vibration of the Muffler/Shock-loop Assembly	139
Figure 6.14	Equivalent Valve Impact Forces	140
Figure 6.15	Equivalent Valve Impact Moments	141

List of Tables

Table 3.1	Sine and Cosine Coefficients of the Force Vectors	30
Table 3.2	Real Components of the Sine and Cosine Coefficients of the Response Vectors	32
Table 3.3	Imaginary Components of the Eigenvalues	37
Table 5.1	Location of Crank-Case and Motor-Cap Accelerometers with Respect to System Origin	78
Table 5.2	Break Points of Periods in the Measured Data	81
Table 5.3	Acceleration Data at the Starting and Ending Point of the First Period	82
Table 6.1	Natural Frequencies of the Original Model of the Compressor with Different ground Spring Stiffnesses K	103

CHAPTER ONE
INTRODUCTION

1.1 Project Overview

This thesis is part of the effort of several teams working on different aspects of the Bristol H25A compressor project. These teams consists of an analytical modeling team, a finite element modeling team, an experimental modal analysis team, and an acoustic analysis team. The project was originally started in January 1993 and ended in August 1995. The subjects that were investigated included (1) prediction of the orbit of the compressor through an analytical model, (2) generation of a force function matrix based on kinematics, (3) gathering experimental data from an operating H25A compressor and verification of the analytical model, (4) construction of a multiple-input/single-output model to identify and rank the transmission paths of sound within the compressor, (5) development of a finite element model and determine the response shapes of the compressor housing, and (6) verification of the finite element model by modal analysis.

New subjects that had been addressed included (1) prediction of acoustic radiation using experimental force transducer inputs, (2) study the effect of change in thickness of shell, (3) study of mass addition on top, (4) study the movement of the side suspensions to alternate positions, (5) study of a stiffener addition to top, (6) study the radiation due to each suspension spring, and (7) study of tuned absorber additions to the lower spring supports below the springs.

The work presented in this thesis focuses on the analytical modeling which predicts the dynamic forces and accelerations of the subassemblies within the compressor. These subassemblies include the crank-case assembly, muffler, and the electric motor and these were connected to the compressor shell through two side springs, one top spring and a shock- loop structure. With the assumption that these subassemblies have rigid-body motion and that the shell has negligible motion compared to the compressor frame, a

system model consisting of four springs and one lumped mass was developed. The kinematic forces due to the slider-crank mechanism have been analyzed and applied to the system to obtain the forced vibration response. This work has been implemented as an integrated compressor analysis program *COMP* using the Visual Basic™ programming language *. *COMP* features a preprocessor for entering the compressor parameters, a processor which performs the computations and a post processor to display the analysis results. The program is a Microsoft® Windows™ * application and adopts standard Windows graphical user interface, along with an on-line help system.

Further work was focused on the experimental data and the finite element model. The first step was the enforced motion excitation analysis. Based on the accelerations measured at two locations within the compressor, the accelerations at the mass center were regenerated through kinematic principles. The accelerations at the mass center were then converted into excitation forces using the penalty method and applied to a finite element model to solve for the responses at the spring ends and these forces were compared with the force gauge measurements. Meanwhile, the forces and moments at the shock loop and the moments at all spring ends which had not been measured are also obtained through this dynamic analysis.

The second step was the forced excitation analysis. The excitation force is the summation of the kinematic force computed by *COMP* and the valve forces generated by a valve simulation program. Meanwhile, the original finite element model was modified with the consideration of the mass and stiffness addition due to the insertion of the force gauges. Both the original model and the instrumental model are studied, with the consideration of local resonances, such as the muffler/shock-loop assembly and the stator.

* *Microsoft® Visual Basic™ Version 3.0 Professional Edition, Microsoft® Windows™ Version 3.1*

1.2 Bristol H25A Compressor

The Bristol H25A compressor is a two-cylinder reciprocating Freon compressor for air conditioning or refrigeration purposes. Its nominal capacity is 61,000 BTUH. The compressor is driven by a three-phase, 5.4 kW electric motor running at 3450 rpm. Figure 1.1 and Figure 1.2 shows the outside view and the internal components of the H25A compressor respectively.

1.3 Previous Analysis Results

The previous analysis results are mainly contributed by Ramakant Arcot [3], Matthew Craun [2] and Anand Ramani [4] during 1993, and Samir Singh [5] in 1994. Arcot created an analytical model of the subassemblies within the compressor and performed the kinematic force analysis and orbit prediction. Arcot's model was that of a two-cylinder compressor elastically mounted to the shell through three springs and the shock-loop. Analyses were performed in three areas, (1) natural frequencies and normal modes, (2) kinematic force analysis and (3) orbit response at the mass center of gravity. The computer program associated with the above model included a FORTRAN program which calculates the kinematic forces at the mass center, a FORTRAN program which performs the eigenanalysis and solves the equation of motion of the system and a PHIGS program which animates the orbit of the compressor mass. The force analysis FORTRAN program has been converted into several Visual Basic™ subroutines within *COMP*.

Craun [2] developed a multiple-input/single-output (MISO) model to analyze the propagation paths of sound within the compressor, and also performed the instrumentation and testing of the H25A compressor. The measurements included the force measurement at the top mount, the left and right mounts in the X, Y and Z directions, the acceleration measurements at the crank-case and motor-cap in the X, Y and Z directions, and the pressure measurements within the top and bottom cylinders, and at the suction and exhaust plenums. Figure 1.3 shows the views of the compressor and a summary of the instrumentation. The plots of the measured data are shown in Chapter 5.

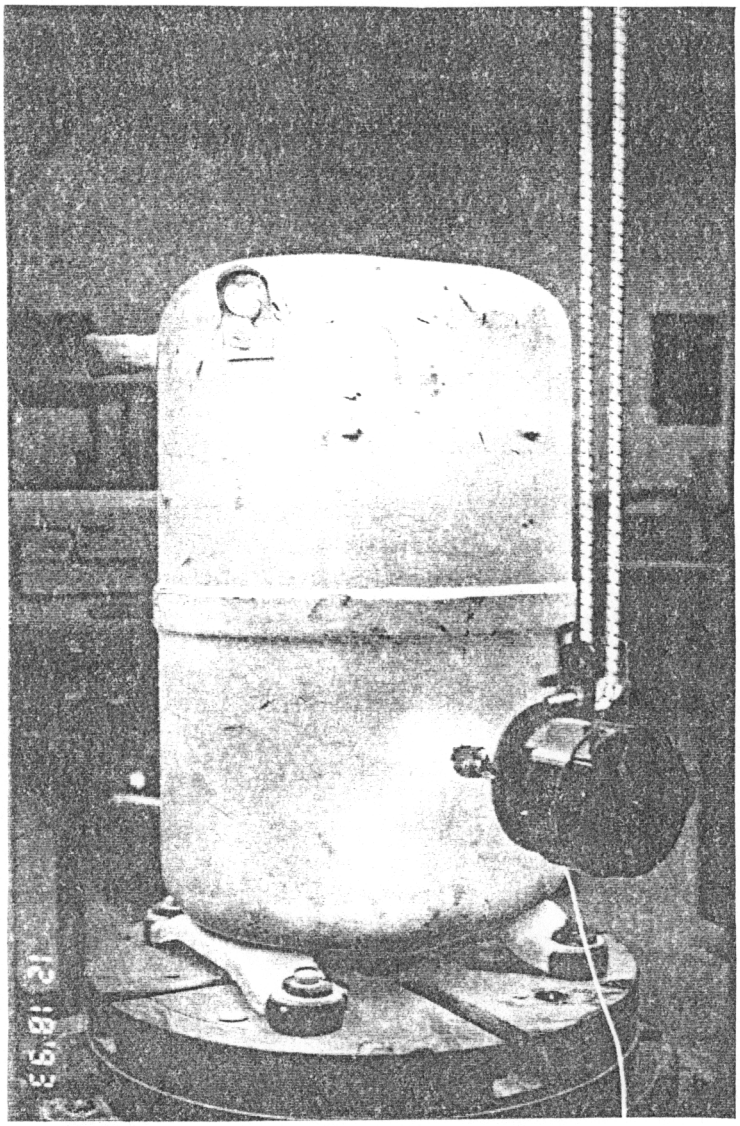

Figure 1.1 The Bristol H25A Compressor (From Rose [1])

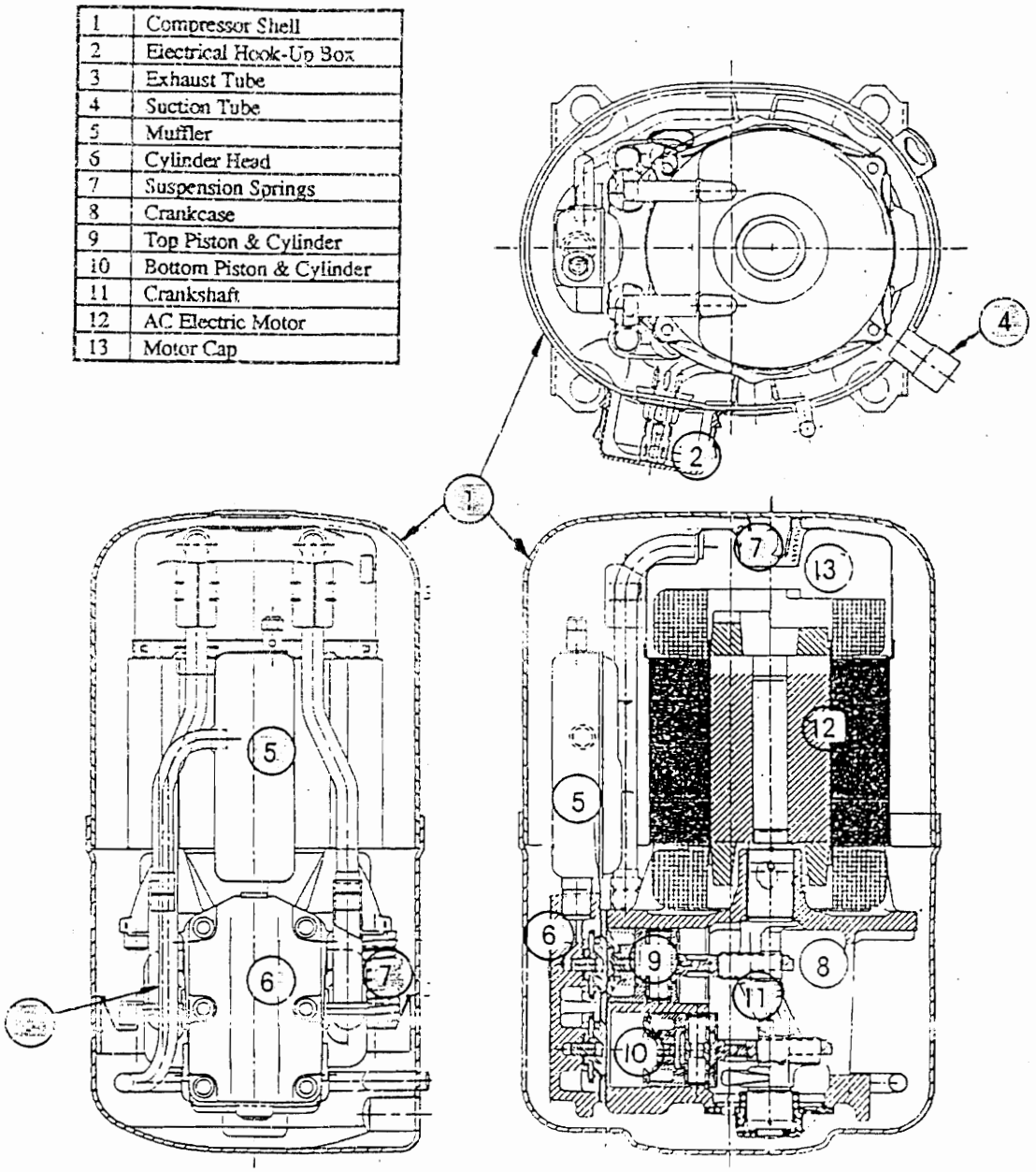

Figure 1.2 Internal Components of the Bristol H25A Compressor (From Craun [2])

1	Right Triaxial Force Transducer
2	Left Triaxial Force Transducer
3	Top Triaxial Force Transducer
4	Shock Loop Accelerometer
5	Housing Pressure Transducer
6	Top Cylinder Pressure Transducer
7	Bottom Cylinder Pressure Transducer
8	Exhaust Pressure Transducer
9	Suction Pressure Transducer
10	Crankshaft Gear
11	Crankcase Accelerometer
12	Motor Cap Accelerometer

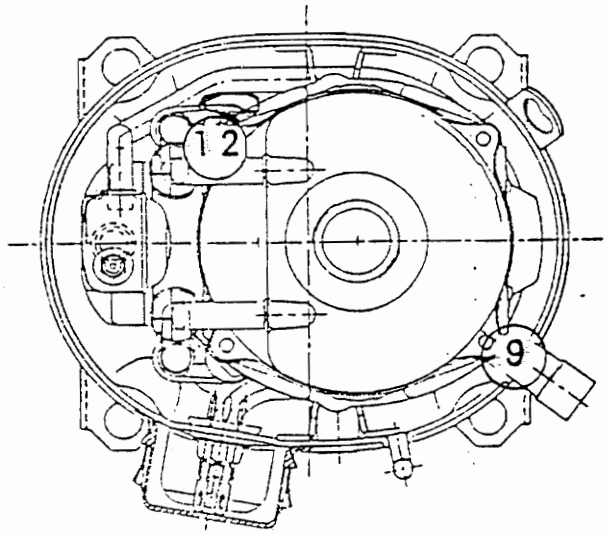

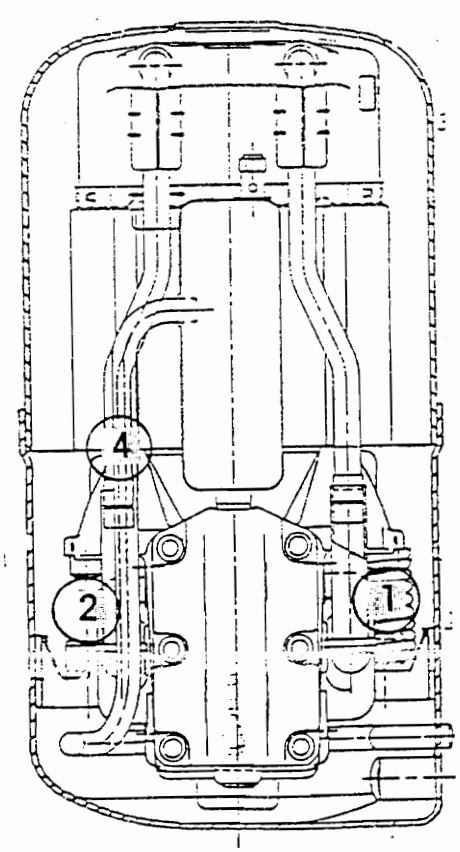

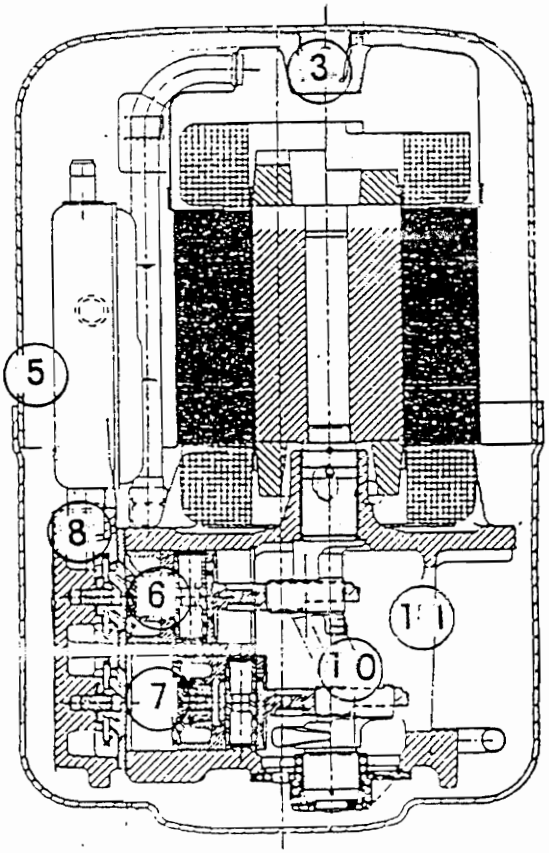

Figure 1.3 The Bristol H25A Compressor Instrumentation (From Craun [2])

The full compressor was modeled using the finite element method by Ramani [4]. Considerable efforts were made on modeling the housing structure. The subassemblies within the housing were modeled as a single lumped mass element except for the springs and the shock loop which were modeled as beams. The natural frequencies obtained from the finite element model were compared with those gathered from modal experiments, and revisions were made in order to reduce the differences between the analytical method and the experimental method to a minimum. In addition, the crank-case had been investigated separately.

The study of Samir Singh [5] is focused on the investigations of pressure fluctuations inside the compressor cavity and their effect on the forces generated by the impact of the valves on the valve seats and valve stops. A computer simulation program was developed for prediction of the cylinder pressures as well as the pressures within various cavities inside the compressor. Singh's program also computes the valve impact forces due to both suction and discharge valves and the results can be imported into *COMP* for further orbit analysis.

CHAPTER TWO
THEORETICAL MODEL

The theoretical model of the H25A compressor is developed in order to ascertain the response at the mass center. Subassemblies within the compressor, including the crank-case, muffler, electric motor, etc., are modeled as a combined single rigid body and attached to the rigid shell through three mounting springs and the shock-loop. This model was first developed by Arcot [3] and was adopted by *COMP*. This chapter briefly describes the modeling procedure, the evaluation of the parameters, and the details are in reference [3].

The modeling follows the procedure:

- Establish the system equations of motion
- Evaluate the parameters in the system equations of motion
- Solve the system equations of motion.

2.1 Establish the System Equations of Motion

The system equations of motion can be determined utilizing the sketch of the compressor model in Figure 2.1. The system shown in Figure 2.1 consists of one lumped mass, three helical springs and a shock-loop. With the assumption that the shell is rigid, one end of the mounting spring can be treated as grounded. The shock-loop also behaves similar to a helical spring. The system equations of motion can be written as:

$$M\ddot{x} + G\dot{x} + Kx = F(t) \tag{2.1}$$

where M is the mass matrix, G is the gyroscopic matrix, K is the system stiffness matrix, F is the shaking force vector. The displacement vector $\mathbf{x}$ is a six-DOF vector, that represents the response at the mass center. The vector includes the translational displacements in the X, Y and Z axes, and the rotational displacements about the X, Y and Z axes. The sizes of these matrices are, therefore, 6×6, and the force vector F also includes both forces and moments.

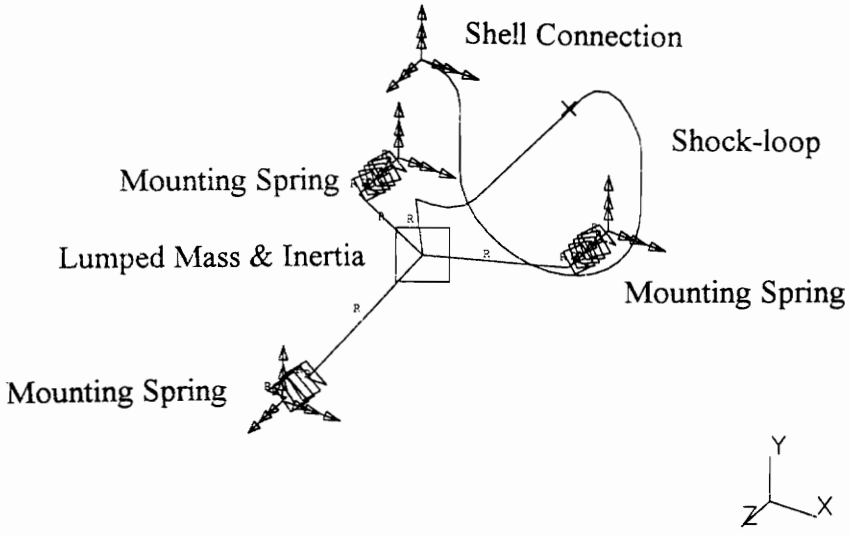

Figure 2.1 A Sketch of the Compressor Model

2.2 Evaluation of the Parameters in the System Equations of Motion

From the equations of motion, the parameters that need to be evaluated are: (1) system mass and inertia matrix, (2) gyroscopic matrix, (3) system stiffness matrix, and (4) the shaking forces and moments vector. The evaluation of these parameters will involve both experimental method and finite element analysis.

2.2.1 System Mass and Inertia Matrix

When constructing the system mass and inertia matrix, the first step is the determination of the center of mass of the assembly. The center of mass also serves as the origin of the coordinate system used for calculating the inertias, forces, moments, and also the responses. The inclined-plane method is used to locate the center of mass of the assembly [3]. With respect to the global coordinate system *, the center of mass is located at

$$(x_o, y_o, z_o) = (0.01,\ -3.51,\ 5.71) \quad \text{(in.)}$$

* *The origin of the global coordinate system in [3] is located at a point where the center line of the bottom cylinder intersects with the outer surface of the cylinder head plate as shown in Figure 2.2. In COMP, the origin is defined at the intersection of the center line of the crank-shaft and the center line of the bottom cylinder.*

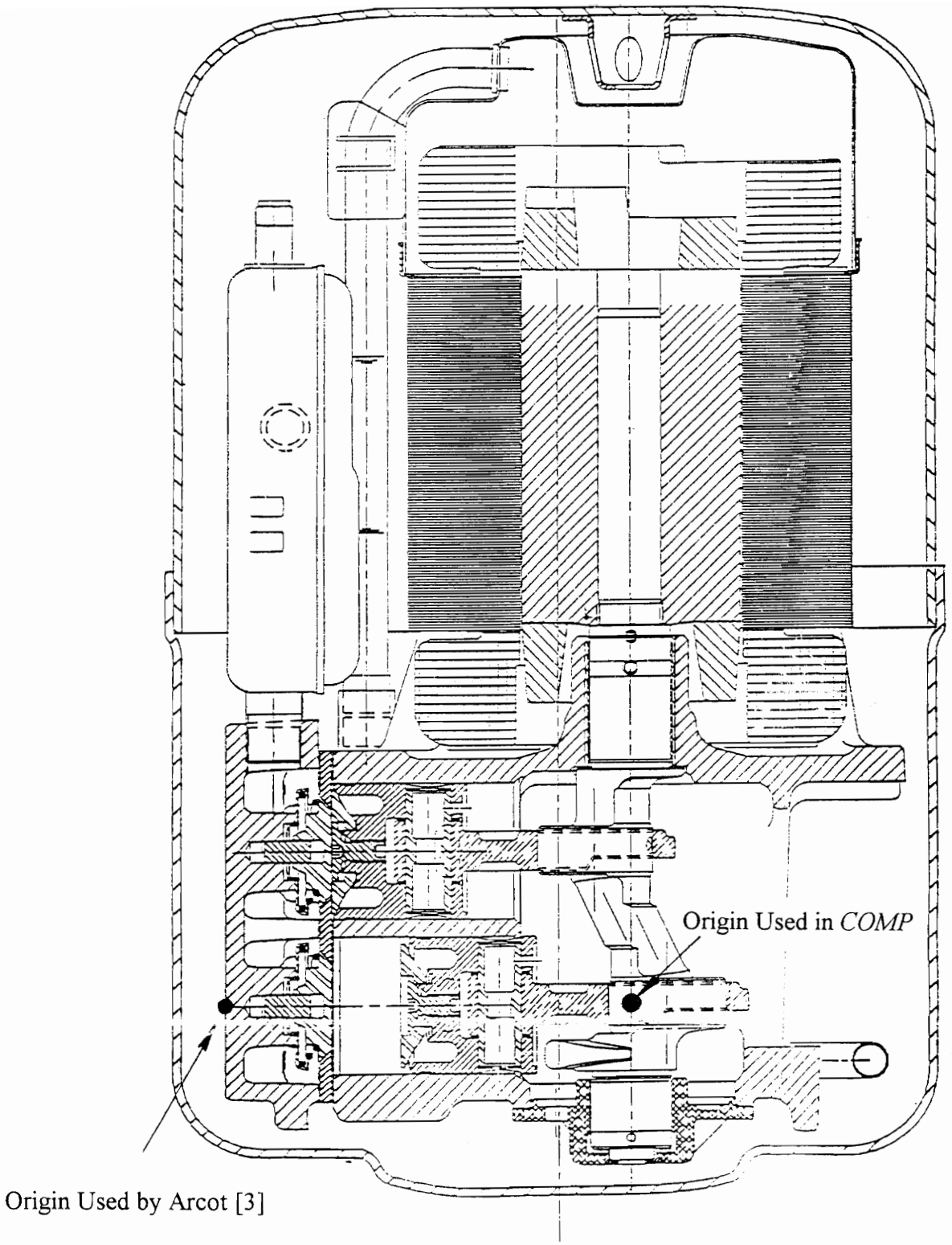

Figure 2.2 Origins of the Coordinate System Used by Arcot [3] and *COMP*

After coordinate transformation, the center of mass in *COMP* is at

$$(x_o, y_o, z_o) = (0.01,\ 0.64,\ 5.71) \qquad \text{(in.)}$$

The weight moment of inertia of the compressor is determined by Arcot [3] and verified by Ramani [4] using the torsional pendulum method discussed by Holman [6] as

$$I_{xx} = 1305 \text{ lb} \cdot \text{in.}^2$$
$$I_{yy} = 1145 \text{ lb} \cdot \text{in.}^2$$
$$I_{zz} = 561 \text{ lb} \cdot \text{in.}^2$$

in terms of mass moment of inertia (lb·in.·sec^2) units, the above inertias can be written as

$$I_{xx} = 3.38 \text{ lb} \cdot \text{in.} \cdot \text{sec}^2$$
$$I_{yy} = 2.97 \text{ lb} \cdot \text{in.} \cdot \text{sec}^2$$
$$I_{zz} = 1.45 \text{ lb} \cdot \text{in.} \cdot \text{sec}^2$$

The product of inertia terms for the compressor were obtained from the solid model by Ramani [4], and are as follows

$$I_{xy} = 0.00 \text{ lb} \cdot \text{in.} \cdot \text{sec}^2$$
$$I_{yz} = -0.49 \text{ lb} \cdot \text{in.} \cdot \text{sec}^2$$
$$I_{zz} = 0.00 \text{ lb} \cdot \text{in.} \cdot \text{sec}^2$$

The weight of the compressor internal assembly is 79.6 lb., which in terms of mass is 0.206 lb·sec^2/in. So the mass and inertia matrix can be written as

$$\boldsymbol{M} = \begin{bmatrix} 0.206 & 0 & 0 & 0 & 0 & 0 \\ 0 & 0.206 & 0 & 0 & 0 & 0 \\ 0 & 0 & 0.206 & 0 & 0 & 0 \\ 0 & 0 & 0 & 3.38 & 0 & 0 \\ 0 & 0 & 0 & 0 & 2.97 & -0.49 \\ 0 & 0 & 0 & 0 & -0.49 & 1.45 \end{bmatrix} \begin{bmatrix} \text{lb} \cdot \text{sec}^2/\text{in.} & \text{lb} \cdot \text{sec}^2/\text{rad} \\ \text{lb} \cdot \text{sec}^2 & \text{lb} \cdot \text{in sec}^2/\text{rad} \end{bmatrix}$$

2.2.2 System Gyroscopic Matrix

The system gyroscopic matrix is determined by a couple of gyroscopic moments due to the high speed rotation of the rotor of the electric motor and the crank-shaft about the

vertical axis. According to Mabie and Ocvirk [7], the gyroscopic moments are calculated by

$$M_x = I_{zz}\dot{\theta}\dot{\theta}_y$$
$$M_y = -I_{zz}\dot{\theta}\dot{\theta}_x \qquad (2.2)$$

where $\dot{\theta}$ is the rotational speed of the rotor and $\dot{\theta}_x$ and $\dot{\theta}_y$ are the rotational speed about the X and Y axes. Thus, the system gyroscopic matrix can be written as

$$G = \begin{bmatrix} 0 & 0 & 0 & 0 & 0 & 0 \\ 0 & 0 & 0 & 0 & 0 & 0 \\ 0 & 0 & 0 & 0 & 0 & 0 \\ 0 & 0 & 0 & 0 & I_{zz}\dot{\theta} & 0 \\ 0 & 0 & 0 & -I_{zz}\dot{\theta} & 0 & 0 \\ 0 & 0 & 0 & 0 & 0 & 0 \end{bmatrix} \qquad (2.3)$$

Again, the torsional pendulum method of Holman [6] is used to ascertain the mass moment of inertia of the rotor with respect to the its axis.

$$I_{zz} = 0.0262 \text{ lb} \cdot \text{in.} \cdot \text{sec}^2$$

At steady state, the rotating speed is 3450 rpm, which is 361.28 rad/sec. Substituting I_{zz} and $\dot{\theta}$ into G, we have the system gyroscopic matrix as

$$G = \begin{bmatrix} 0 & 0 & 0 & 0 & 0 & 0 \\ 0 & 0 & 0 & 0 & 0 & 0 \\ 0 & 0 & 0 & 0 & 0 & 0 \\ 0 & 0 & 0 & 0 & 9.45 & 0 \\ 0 & 0 & 0 & -9.45 & 0 & 0 \\ 0 & 0 & 0 & 0 & 0 & 0 \end{bmatrix} \quad \begin{bmatrix} \text{lb} \cdot \text{sec/in.} & \text{lb} \cdot \text{sec/rad} \\ \text{lb} \cdot \text{sec} & \text{lb} \cdot \text{in.} \cdot \text{sec/rad} \end{bmatrix}$$

2.2.3 System Stiffness Matrix

The system stiffness matrix is constructed based on the information for each of the individual springs, which includes the position of the attachment point of the spring to the shell and the stiffness matrix of each spring. The position of the attachment point is determined by the coordinates in a Cartesian coordinate system, where the origin lies at the center of mass of the compressor. The element stiffness matrix for each individual spring is a 6×6 matrix, including the stiffnesses in all six directions.

The coordinates of the four attachment points as measured by Arcot [3] are as follows:

- Top Spring: $(x_t, y_t, z_t) = (-0.010, -0.93, 7.43)$ (in.)
- Left Spring: $(x_l, y_l, z_l) = (3.18, -0.27, -2.48)$ (in.)
- Right Spring: $(x_r, y_r, z_r) = (-3.18, -0.27, -2.48)$ (in.)
- Shock-Loop: $(x_s, y_s, z_s) = (1.11, 4.14, 2.48)$ (in.)

and the local stiffness matrix of each individual spring is computed by Arcot [3] as

- Top Spring:

$$\boldsymbol{K}_t = \begin{bmatrix} 136 & 0 & 0 & 0 & 1015 & 126 \\ & 136 & 0 & -1015 & 0 & -1.41 \\ & & 100 & -92.5 & 1.03 & 0 \\ & & & 7808 & -0.953 & 10.5 \\ & & & & 7723 & 939 \\ \textit{Symmetric} & & & & & 117 \end{bmatrix}$$

- Left and Right Springs:

$$\boldsymbol{K}_l = \boldsymbol{K}_r = \begin{bmatrix} 562 & 0 & 0 & 0 & -1394 & 151 \\ & 562 & 0 & 1394 & 0 & -1798 \\ & & 450 & -121 & 1439 & 0 \\ & & & 4413 & -387 & -4458 \\ & & & & 8983 & -375 \\ \textit{Symmetric} & & & & & 5791 \end{bmatrix}$$

- Shock-Loop:

$$\boldsymbol{K}_s = \begin{bmatrix} 66.6 & 18.9 & 14.1 & 102 & -351 & -43.5 \\ & 94.3 & 36.4 & 474 & -141 & 110 \\ & & 79.2 & 220 & -169 & 32.9 \\ & & & 6410 & -900 & 300 \\ & & & & 5240 & -2196 \\ \textit{Symmetric} & & & & & 2862 \end{bmatrix}$$

The system stiffness matrix is then assembled as

$$K_{System} = \begin{bmatrix} 1327 & 18.9 & 14.1 & 101 & -2124 & 285 \\ & 1354 & 36.4 & 2247 & -141 & -3487 \\ & & 1079 & -115 & 2710 & 32.9 \\ & & & 23043 & -1675 & -8605.5 \\ & & & & 30929 & -2007 \\ Symmetric & & & & & 14561 \end{bmatrix}$$

Units for the stiffness matrix are

$$\begin{bmatrix} lb/in. & lb/rad \\ lb & lb \cdot in./rad \end{bmatrix}$$

2.2.4 Shaking Forces and Moments Vector

The total shaking forces and moments vector, $F_{shaking}$, is the summation of the reactive forces and moments vector, the torque effect vector, and the counter-weight forces and moments vector.

$$F_{shaking} = F_{reactive} + F_{torque} + F_{counter-weight} \qquad (2.4)$$

The subroutines for calculating the forces and moments are converted from the FORTRAN programs into a Visual Basic™ module *FORCEANA.BAS*. There are four subroutines in the module which are:

- COMPR Computes the forces and moments due to reaction
- CWFM Computes the forces and moments due to the counter-weight
- LOAD1 Computes the torque
- FORCE Performs the Fast Fourier Transform to transform the force into the frequency domain.

The details on the force analysis and calculation are discussed in Arcot's thesis [3].

2.3 Solution of the System Equations of Motion

The system equations of motion consists of six coupled first-order ordinary differential equations. When the gyroscopic matrix is negligible, the modal matrix method can be applied to decouple the coupled equations of motion of the six-DOF system into six uncoupled SDOF equations. However, when the gyroscopic matrix is present, the modal

matrix method can not be applied since the gyroscopic matrix is skew symmetric and not proportional to the mass and stiffness matrices. In this case, the state vector method is introduced to solve the system in the state space. The state vector contains both displacement and velocity information. Chapter Three illustrates the details on the state vector method and the modal matrix method.

CHAPTER THREE
PROCESSOR

The processor part of *COMP* solves for the compressor model created based on the parameters entered in the preprocessor. There are several different tasks undertaken during the model solution phase. First, an eigenvalue/eigenvector analysis is performed to calculate the natural frequencies and their associated mode shapes. Then, the kinematic forces and moments are analyzed and applied to the mass center. The dynamic responses at the mass center are then obtained by solving the equations of motion.

All these tasks are accomplished through various subroutines in *COMP*. Some commonly used subroutines, such as the eigen-analysis subroutines and the *Fast Fourier Transform* subroutines are available from many sources. Others are user-defined subroutines and must be developed based on the kinematics, vibration, or mathematics principles.

This chapter also describes the kinematic, vibration, and mathematics principles used in the program.

3.1 Eigenvalue and Eigenvector Problems

3.1.1. Natural Frequencies and Normal Modes

The equations of motion for an N-DOF vibration system can be derived by Lagrange's equation and has the matrix form of

$$\boldsymbol{M}\ddot{\boldsymbol{x}} + (\boldsymbol{G} + \boldsymbol{C})\dot{\boldsymbol{x}} + \boldsymbol{K}\boldsymbol{x} = \boldsymbol{F} \qquad (3.1.1)$$

where $\boldsymbol{M}$ is known as the mass matrix or inertia matrix, $\boldsymbol{C}$ is called the viscous damping matrix and $\boldsymbol{K}$ is the stiffness matrix. These matrices are $N \times N$ real symmetric matrices. Matrix $\boldsymbol{G}$ is referred as the gyroscopic matrix and is skew symmetric. Vector $\boldsymbol{F}$ is the generalized force vector.